Supplementary Information

Merging dynamical and structural indicators to measure resilience in multispecies systems

Lucas P. Medeiros[1*], Chuliang Song[1,2,3*], Serguei Saavedra[1†]

[1]Department of Civil and Environmental Engineering, MIT,
77 Massachusetts Av., 02139 Cambridge, MA, USA
[2]Department of Biology, Quebec Centre for Biodiversity Science, McGill University,
Montreal, Canada H3A 1B1
[3]Department of Ecology and Evolutionary Biology, University of Toronto,
25 Willcocks Street, Toronto, Ontario M5S 3B2 Canada

*Equal contribution

†To whom correspondence should be addressed. E-mail: sersaa@mit.edu ORCID 0000-0003-1768-363X

	r_i
Ea	0.46
Pa	0.55
Pch	0.18
Pci	0.16
Pf	0.25
Pp	0.65
Pv	0.57
Sm	0.34

Table S1: Experimentally parameterized growth rates r_i from Friedman *et al.* (2017). Note that the parameterization follows the r-formalism (Equation (1) in the main text). Species names: *Enterobacter aerogenes* (Ea), *Pseudomonas aurantiaca* (Pa), *Pseudomonas chlororaphis* (Pch), *Pseudomonas citronellolis* (Pci), *Pseudomonas fluorescens* (Pf), *Pseudomonas putida* (Pp), *Pseudomonas veronii* (Pv), and *Serratia marcescens* (Sm).

	Ea	Pa	Pch	Pci	Pf	Pp	Pv	Sm
Ea	-3.54	-2.44	-3.86	-1.95	-5.41	-2.90	-3.86	-2.55
Pa	1.41	-7.86	-19.17	20.27	-8.88	-3.38	-0.08	-1.65
Pch	0.18	1.31	-1.64	25.77	-0.47	0.07	0.08	0.05
Pci	5.12	-0.00	-2.88	-16.00	54.24	-0.00	-0.80	4.80
Pf	0.10	-1.40	-6.00	-4.15	-5.00	-0.05	-0.35	0.50
Pp	-4.04	-7.34	-5.76	-1.11	-4.64	-4.64	-4.69	-3.90
Pv	-4.30	-1.45	-2.44	-0.00	0.10	-4.09	-5.18	-3.63
Sm	-2.18	-2.79	-3.22	-2.74	-2.97	-2.06	-2.22	-2.27

Table S2: Experimentally parameterized intra and interspecific interaction strengths a_{ij} from Friedman *et al.* (2017). Note that a_{ij} represents the per capita effect of species j (column) on species i (row) and the parameterization follows the r-formalism (Equation (1) in the main text). Species names are the same as in Table S1.

system	species 1	species 2	species 3
1	Ea	Pp	Sm
2	Pci	Pf	Pv
3	Ea	Pa	Pf
4	Ea	Pa	Pci
5	Pci	Pf	Pp
6	Pci	Pf	Sm
7	Pa	Pci	Pf
8	Pci	Pv	Sm
9	Pa	Pci	Pv
10	Pa	Pf	Pv
11	Pa	Pci	Sm
12	Ea	Pci	Pf
13	Ea	Pci	Pp
14	Ea	Pci	Pv
15	Pci	Pp	Sm
16	Pf	Pp	Sm
17	Pci	Pp	Pv

Table S3: Feasible and dynamically stable 3-species systems chosen from the pool of 8 species in Table S2. These systems are numbered following Figure 5 in the main text and species names are the same as in Table S1.

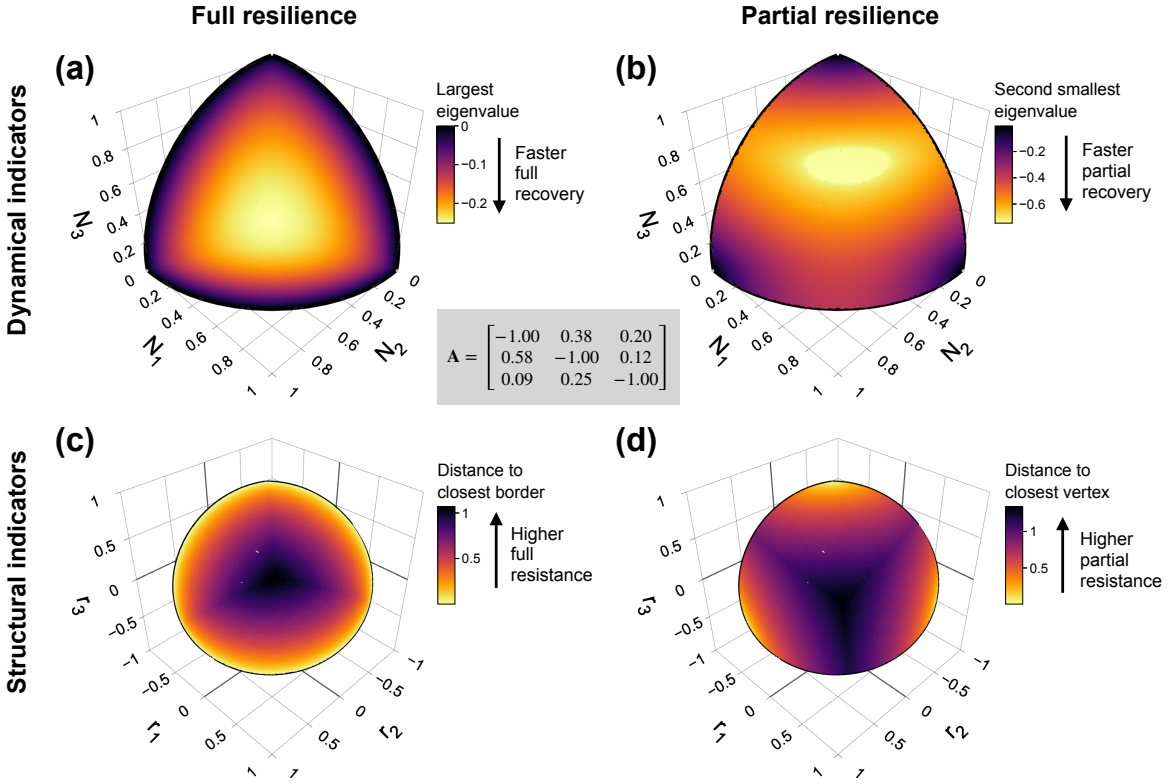

Figure S1: Dynamical and structural indicators of full and partial resilience in a mutualistic system. **(a)** An illustrative example of a 3-dimensional space of species abundances at equilibrium ($\mathbf{N}^*$) colored according to the largest eigenvalue of the Jacobian matrix (λ_1). The interaction matrix $\mathbf{A}$ of this 3-species mutualistic system is shown in the center of the figure. Note that this space corresponds to the positive orthant of the unit sphere (i.e., $||\mathbf{N}^*|| = 1$, $N_i^* > 0 \ \forall \ i$). **(b)** The same space of species abundances, but colored according to the second smallest eigenvalue of the Jacobian matrix (λ_2). **(c)** The space of intrinsic growth rates ($\mathbf{r}$) for the same system shown in (a) and (b) colored according to the distance to closest border ($\min\{d_b\}$) of the feasibility domain, which are indicated as black curves. Note that $\mathbf{r}$-vectors on the feasibility domain are normalized to unit norm (i.e., $||\mathbf{r}|| = 1$). **(d)** The same space of intrinsic growth rates, but colored according to the distance to closest vertex ($\min\{d_v\}$) of the feasibility domain.

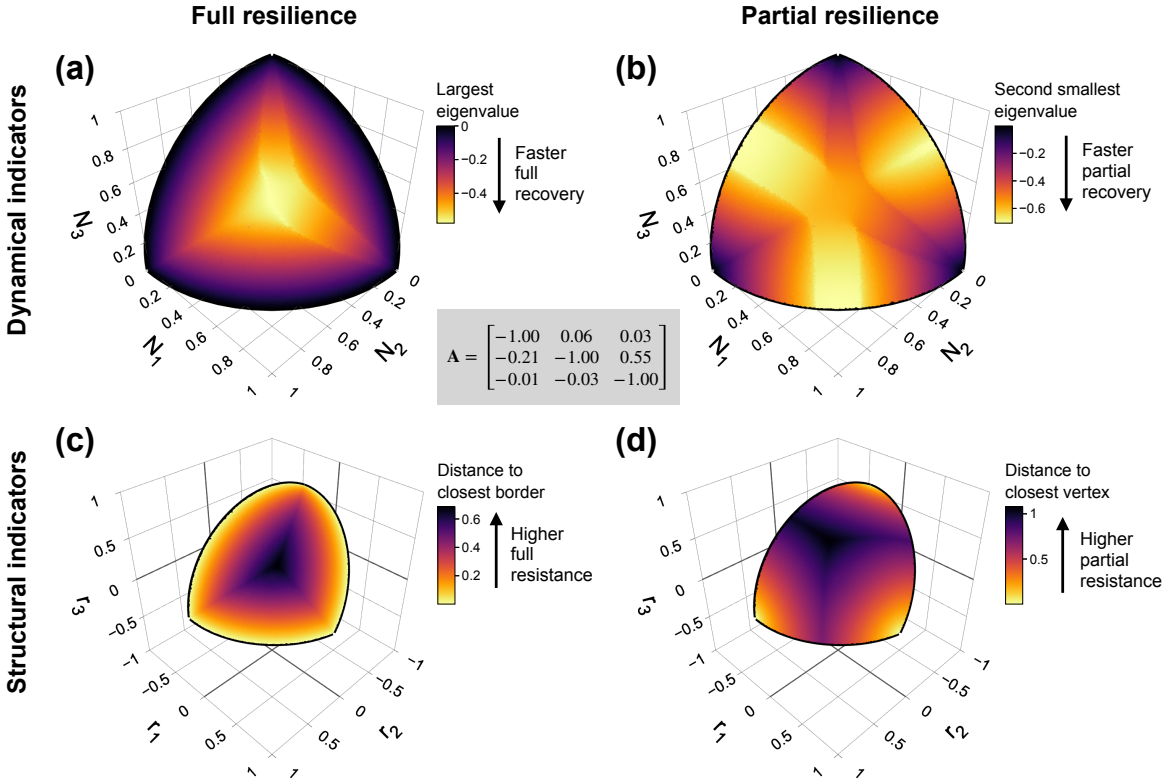

Figure S2: Dynamical and structural indicators of full and partial resilience in an antagonistic system. **(a)** An illustrative example of a 3-dimensional space of species abundances at equilibrium ($\mathbf{N}^*$) colored according to the largest eigenvalue of the Jacobian matrix (λ_1). The interaction matrix $\mathbf{A}$ of this 3-species antagonistic system is shown in the center of the figure. Note that this space corresponds to the positive orthant of the unit sphere (i.e., $||\mathbf{N}^*|| = 1$, $N_i^* > 0 \; \forall \; i$). **(b)** The same space of species abundances, but colored according to the second smallest eigenvalue of the Jacobian matrix (λ_2). **(c)** The space of intrinsic growth rates ($\mathbf{r}$) for the same system shown in (a) and (b) colored according to the distance to closest border ($\min\{d_b\}$) of the feasibility domain, which are indicated as black curves. Note that $\mathbf{r}$-vectors on the feasibility domain are normalized to unit norm (i.e., $||\mathbf{r}|| = 1$). **(d)** The same space of intrinsic growth rates, but colored according to the distance to closest vertex ($\min\{d_v\}$) of the feasibility domain.

	Competition system			Mutualistic system			Antagonistic system		
Correlation	3	4	5	3	4	5	3	4	5
$\rho(\lambda_1, \min\{d_b\})$	-0.98 ± 0.01	-0.98 ± 0.01	-0.94 ± 0.02	-0.91 ± 0.07	-0.89 ± 0.06	-0.80 ± 0.09	-0.97 ± 0.02	-0.97 ± 0.02	-0.94 ± 0.01
$\rho(\lambda_{S-1}, \min\{d_v\})$	-0.90 ± 0.06	-0.82 ± 0.05	-0.74 ± 0.05	-0.77 ± 0.15	-0.78 ± 0.10	-0.74 ± 0.07	-0.77 ± 0.10	-0.65 ± 0.10	-0.55 ± 0.07

Table S4: Mean ($\pm$ standard deviation) correlation between full recovery (largest eigenvalue, λ_1) and full resistance (distance to closest border, $\min\{d_b\}$) as well as between partial recovery (second smallest eigenvalue, λ_{S-1}) and partial resistance (distance to closest vertex, $\min\{d_v\}$). These correlation values correspond to Figures 2b and 3b from the main text. Each mean and standard deviation was computed over 100 theoretical random systems for each combination of system type (competition, mutualistic, and antagonistic system) and size ($S = 3$, 4, and 5). Note that all mean correlation values are strong and negative (≤ -0.55).

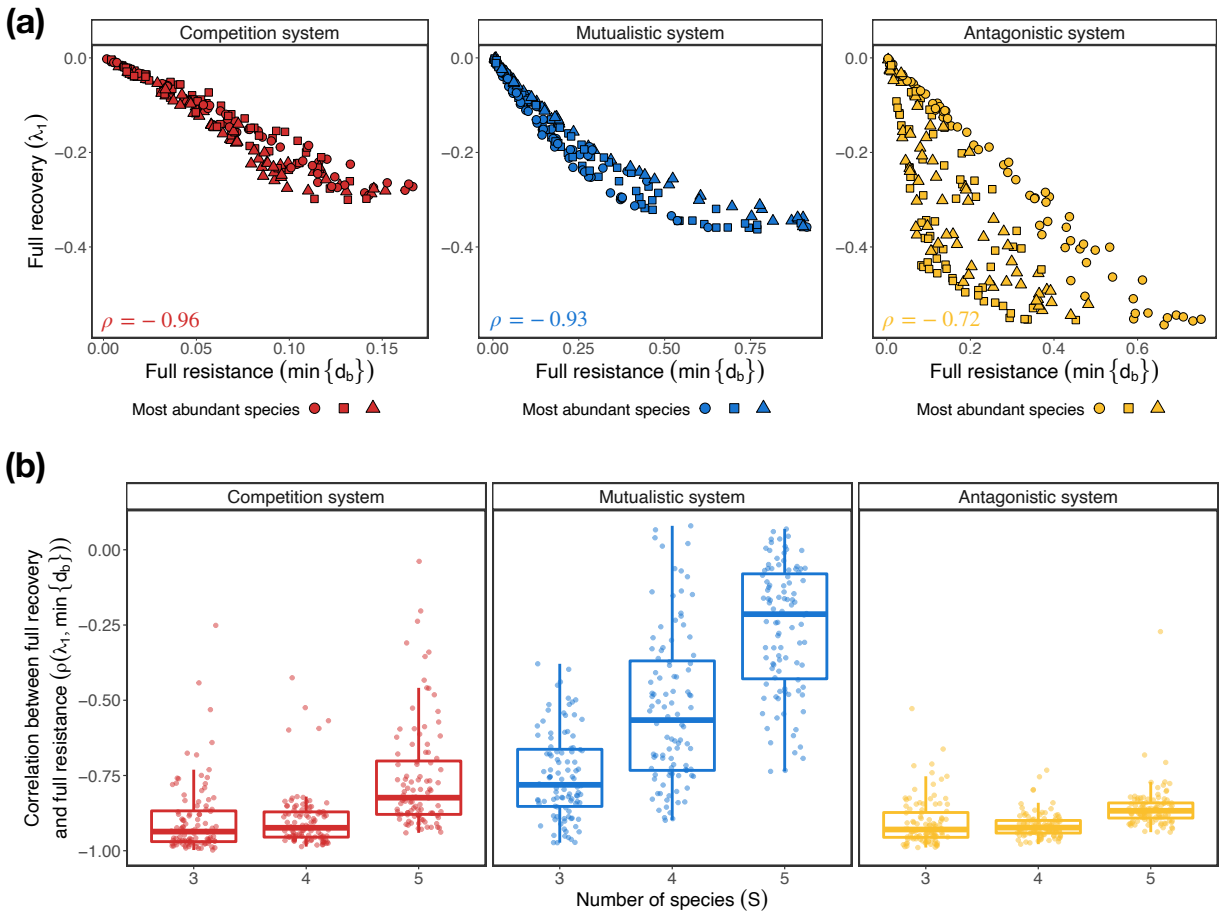

Figure S3: Relationship between full recovery and full resistance in theoretical systems with strong interspecific interactions (i.e., $\sigma^2 = \frac{1}{S}$). **(a)** Each panel shows 200 values of full recovery (largest eigenvalue, λ_1) and full resistance (distance to closest border, $\min\{d_b\}$) of one illustrative theoretical random system with three species (red: competition system, blue: mutualistic system, and yellow: antagonistic system). Point shapes (circle, square, and triangle) correspond to the species with the highest abundance at that equilibrium state. Correlation values between λ_1 and $\min\{d_b\}$ are shown in the bottom left corner of each panel. **(b)** Each panel shows the correlation values between λ_1 and $\min\{d_b\}$ for a given type of system and for three system sizes ($S = 3$, 4, and 5). Boxplots denote the median and interquartile range and points show the actual correlation values obtained for each system type and size (100 values per boxplot).

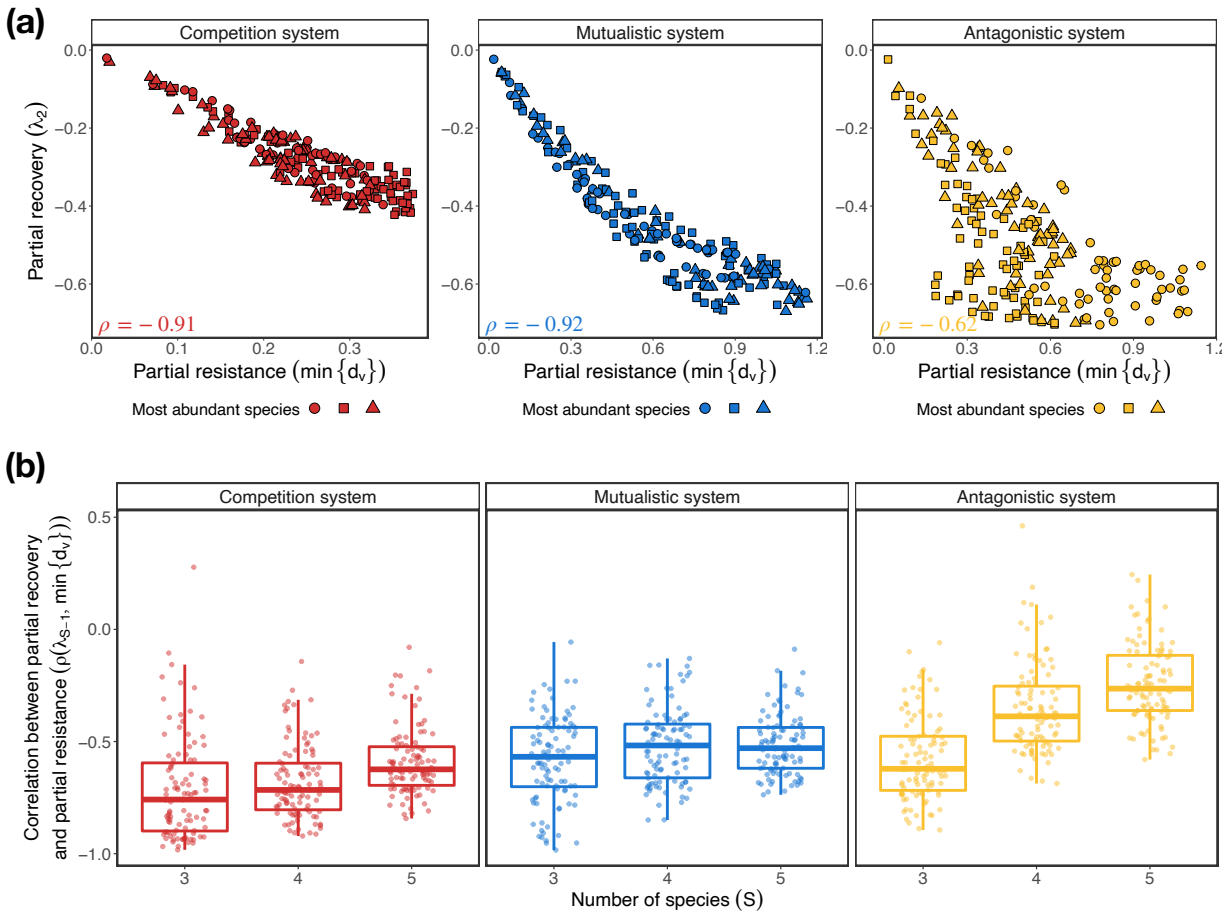

Figure S4: Relationship between partial recovery and partial resistance in theoretical systems with strong interspecific interactions (i.e., $\sigma^2 = \frac{1}{S}$). **(a)** Each panel shows 200 values of partial recovery (second smallest eigenvalue, λ_2) and partial resistance (distance to closest vertex, $\min\{d_v\}$) of the same illustrative theoretical random systems with three species shown in Figure S3 (red: competition system, blue: mutualistic system, and yellow: antagonistic system). Point shapes (circle, square, and triangle) correspond to the species with the highest abundance at the equilibrium state. Correlation values between λ_2 and $\min\{d_v\}$ are shown in the bottom left corner of each panel. **(b)** Each panel shows the correlation values between λ_{S-1} and $\min\{d_v\}$ for a given type of system and for three system sizes ($S = 3$, 4, and 5). Boxplots denote the median and interquartile range and points show the actual correlation values obtained for each system type and size (100 values per boxplot).

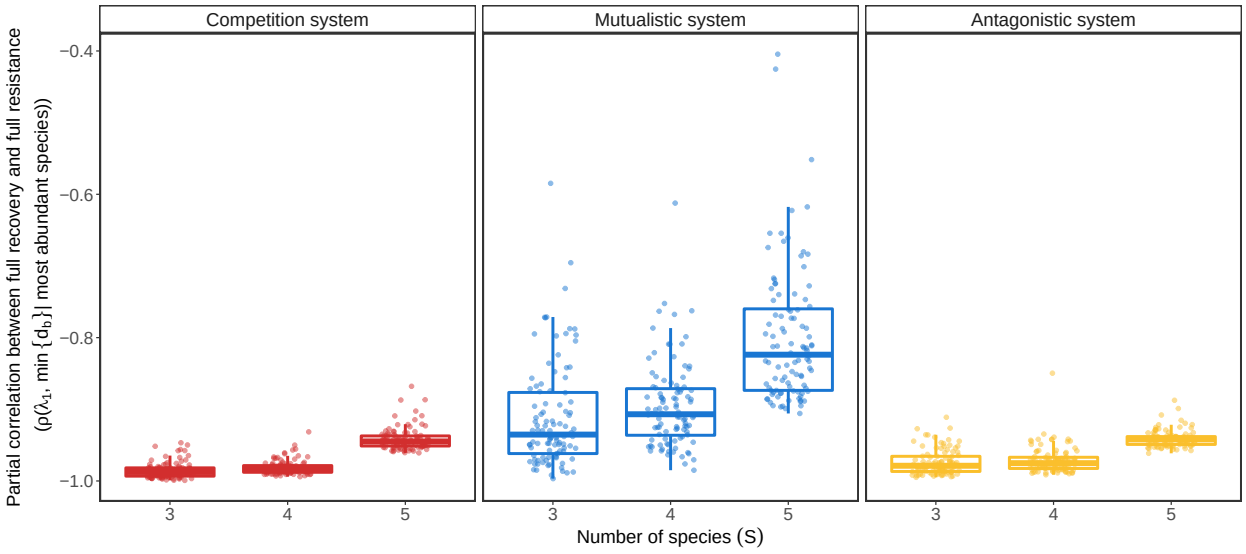

Figure S5: Partial correlation between full recovery and full resistance controlling for the most abundant species in theoretical random systems. Each panel shows the partial correlation values between full recovery (largest eigenvalue, λ_1) and full resistance (distance to closest border, $\min\{d_b\}$) while controlling for the identity of the most abundant species at equilibrium ($\rho(\lambda_1, \min\{d_b\} \mid \text{most abundant species})$) for a given type of system (red: competition system, blue: mutualistic system, and yellow: antagonistic system) and for three system sizes ($S = 3$, 4, and 5). Boxplots denote the median and interquartile range and points show the actual partial correlation values obtained for each system type and size (100 values per boxplot).

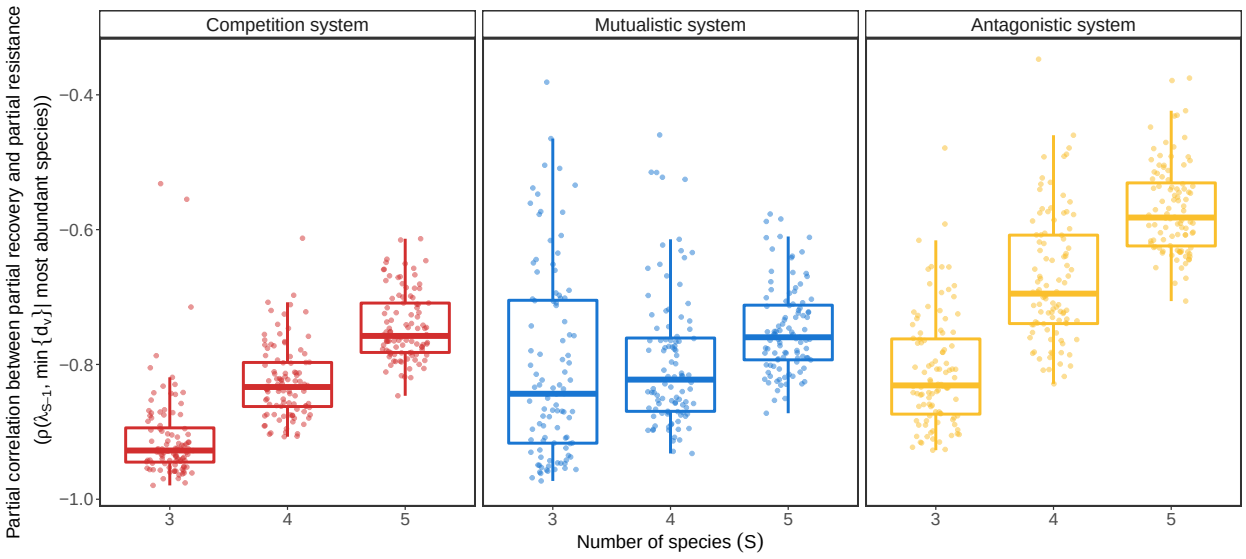

Figure S6: Partial correlation between partial recovery and partial resistance controlling for the most abundant species in theoretical random systems. Each panel shows the partial correlation values between partial recovery (second smallest eigenvalue, λ_{S-1}) and partial resistance (distance to closest vertex, $\min\{d_v\}$) while controlling for the identity of the most abundant species at equilibrium ($\rho(\lambda_{S-1}, \min\{d_v\} \mid \text{most abundant species})$) for a given type of system (red: competition system, blue: mutualistic system, and yellow: antagonistic system) and for three system sizes ($S = 3$, 4, and 5). Boxplots denote the median and interquartile range and points show the actual partial correlation values obtained for each system type and size (100 values per boxplot).

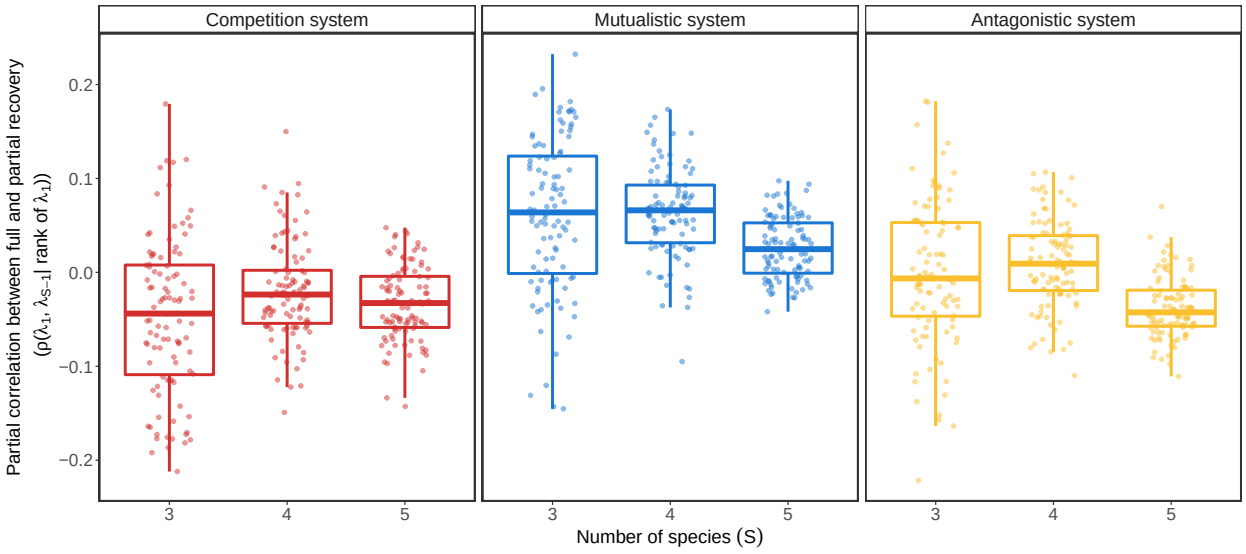

Figure S7: Partial correlation between full and partial recovery controlling for rank in theoretical random systems. Each panel shows the partial correlation values between full recovery (largest eigenvalue, λ_1) and partial recovery (second smallest eigenvalue, λ_{S-1}) while controlling for the rank of λ_1 ($\rho(\lambda_1, \lambda_{S-1} \mid \text{rank of } \lambda_1)$) for a given type of system (red: competition system, blue: mutualistic system, and yellow: antagonistic system) and for three system sizes ($S = 3$, 4, and 5). Note that these partial correlation values are expected to be close to zero. Boxplots denote the median and interquartile range and points show the actual partial correlation values obtained for each system type and size (100 values per boxplot).

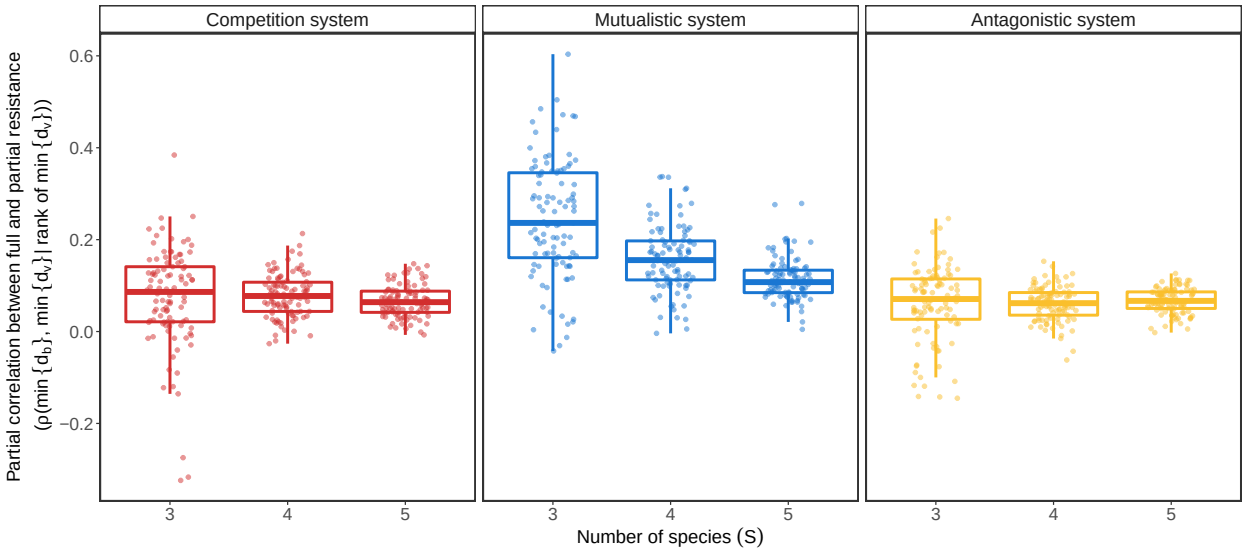

Figure S8: Partial correlation between full and partial resistance controlling for rank in theoretical random systems. Each panel shows the partial correlation values between full resistance (distance to closest border, $\min\{d_b\}$) and partial resistance (distance to closest vertex, $\min\{d_v\}$) while controlling for the rank of $\min\{d_v\}$ ($\rho(\min\{d_b\}, \min\{d_v\} \mid \text{rank of } \min\{d_v\})$) for a given type of system (red: competition system, blue: mutualistic system, and yellow: antagonistic system) and for three system sizes ($S = 3$, 4, and 5). Note that these partial correlation values are expected to be close to zero. Boxplots denote the median and interquartile range and points show the actual partial correlation values obtained for each system type and size (100 values per boxplot).

	Competition system			Mutualistic system			Antagonistic system		
Partial correlation	3	4	5	3	4	5	3	4	5
$\rho(\lambda_1, \min\{d_b\} \mid$ most abundant species$)$	-0.99 ± 0.01	-0.98 ± 0.01	-0.94 ± 0.02	-0.91 ± 0.07	-0.89 ± 0.06	-0.80 ± 0.09	-0.97 ± 0.02	-0.97 ± 0.02	-0.94 ± 0.01
$\rho(\lambda_{S-1}, \min\{d_v\} \mid$ most abundant species$)$	-0.91 ± 0.07	-0.82 ± 0.05	-0.74 ± 0.05	-0.80 ± 0.14	-0.80 ± 0.10	-0.75 ± 0.06	-0.81 ± 0.08	-0.67 ± 0.09	-0.57 ± 0.07
$\rho(\lambda_1, \lambda_{S-1} \mid$ rank of $\lambda_1)$	-0.05 ± 0.08	-0.02 ± 0.05	-0.03 ± 0.04	0.06 ± 0.08	0.06 ± 0.05	0.03 ± 0.03	-0.002 ± 0.08	0.009 ± 0.05	-0.04 ± 0.03
$\rho(\min\{d_b\}, \min\{d_v\} \mid$ rank of $\min\{d_v\})$	0.07 ± 0.11	0.08 ± 0.05	0.07 ± 0.03	0.24 ± 0.13	0.16 ± 0.07	0.11 ± 0.04	0.06 ± 0.08	0.06 ± 0.04	0.07 ± 0.03

Table S5: Mean ($\pm$ standard deviation) partial correlations. The first and second rows show the partial correlation between full recovery (largest eigenvalue, λ_1) and full resistance (distance to closest border, $\min\{d_b\}$) as well as between partial recovery (second smallest eigenvalue, λ_{S-1}) and partial resistance (distance to closest vertex, $\min\{d_v\}$) while controlling for the identity of the most abundant species at equilibrium. Note that all mean partial correlation values in these two rows are strong and negative (≤ -0.57), similarly to Table S4. These partial correlation values correspond to Figures S5 and S6. The third and fourth rows show the partial correlation between full recovery (largest eigenvalue, λ_1) and partial recovery (second smallest eigenvalue, λ_{S-1}) as well as between full resistance (distance to closest border, $\min\{d_b\}$) and partial resistance (distance to closest vertex, $\min\{d_v\}$) while controlling for the rank of the largest variable (i.e., λ_1 or $\min\{d_v\}$). Note that most mean partial correlation values in these two rows are close to 0, showing that these indicators are complementary. These partial correlation values correspond to Figures S7 and S8. Each mean and standard deviation was computed over 100 random systems for each combination of system type (competition, mutualistic, and antagonistic system) and size ($S = 3$, 4, and 5).

Correlation	Value
$\rho(\lambda_1, \min\{d_b\})$	-0.69 ± 0.23
$\rho(\lambda_2, \min\{d_v\})$	-0.56 ± 0.23

Table S6: Mean ($\pm$ standard deviation) correlation between full recovery (largest eigenvalue, λ_1) and full resistance (distance to closest border, $\min\{d_b\}$) as well as between partial recovery (second smallest eigenvalue, λ_2) and partial resistance (distance to closest vertex, $\min\{d_v\}$) for the 3-species experimental microbial systems. Each mean and standard deviation was computed over the 17 experimental systems. As expected, both mean correlation values are strong and negative.

Partial correlation	Value
$\rho(\lambda_1, \min\{d_b\} \mid \text{most abundant species})$	-0.70 ± 0.24
$\rho(\lambda_2, \min\{d_v\} \mid \text{most abundant species})$	-0.53 ± 0.24
$\rho(\lambda_1, \lambda_2 \mid \text{rank of } \lambda_1)$	-0.13 ± 0.19
$\rho(\min\{d_b\}, \min\{d_v\} \mid \text{rank of } \min\{d_v\})$	0.07 ± 0.18

Table S7: Mean ($\pm$ standard deviation) partial correlations for the 3-species experimental microbial systems. The first and second rows show the partial correlation between full recovery (largest eigenvalue, λ_1) and full resistance (distance to closest border, $\min\{d_b\}$) as well as between partial recovery (second smallest eigenvalue, λ_2) and partial resistance (distance to closest vertex, $\min\{d_v\}$) while controlling for the identity of the most abundant species at equilibrium. Note that the mean partial correlation values in these two rows are strong and negative, similarly to Table S6. The third and fourth rows show the partial correlation between full recovery (largest eigenvalue, λ_1) and partial recovery (second smallest eigenvalue, λ_2) as well as between full resistance (distance to closest border, $\min\{d_b\}$) and partial resistance (distance to closest vertex, $\min\{d_v\}$) while controlling for the rank of the largest variable (i.e., λ_1 or $\min\{d_v\}$). Note that the mean partial correlation values in these two rows are close to zero, confirming the complementarity between these indicators. Each mean and standard deviation was computed over the 17 experimental systems.

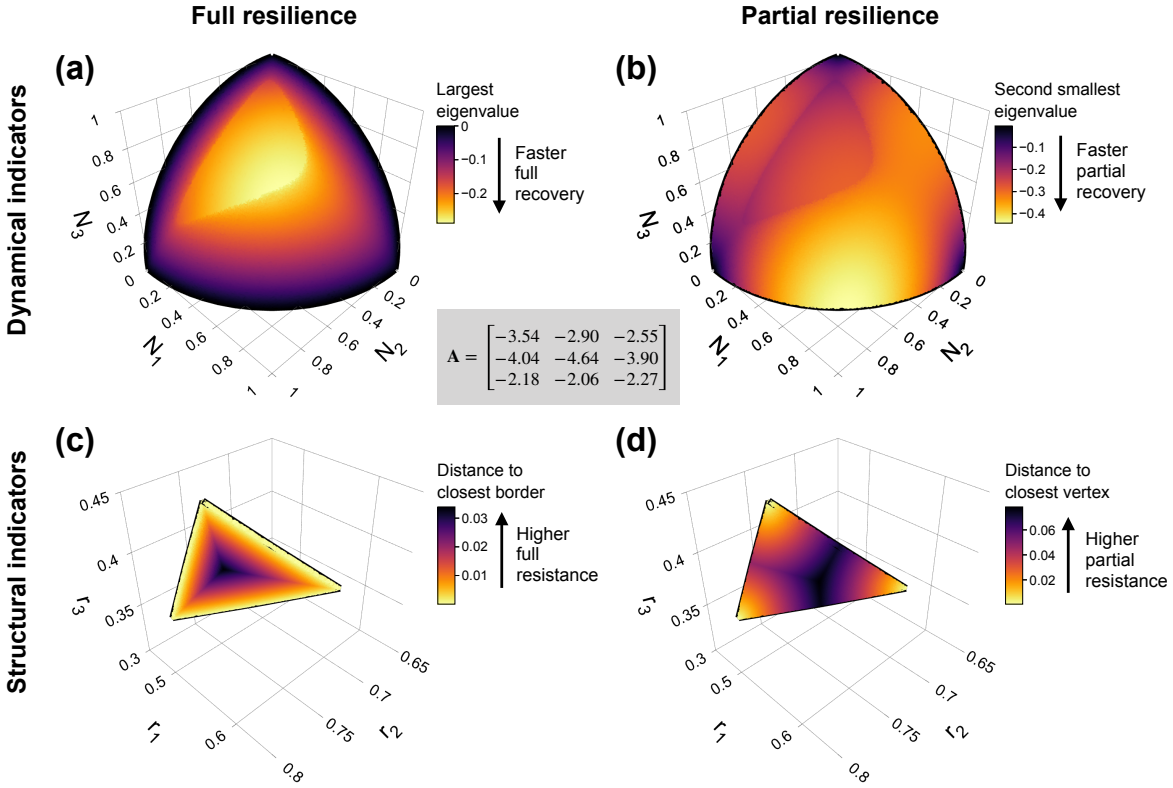

Figure S9: Dynamical and structural indicators of full and partial resilience in a competition microbial system (system 1: Ea-Pp-Sm; Tables S1 and S3). **(a)** The 3-dimensional space of species abundances at equilibrium ($\mathbf{N}^*$) colored according to the largest eigenvalue of the Jacobian matrix (λ_1). The interaction matrix $\mathbf{A}$ of this 3-species system is shown in the center of the figure. Note that this space corresponds to the positive orthant of the unit sphere (i.e., $||\mathbf{N}^*|| = 1$, $N_i^* > 0 \; \forall \; i$). **(b)** The same space of species abundances, but colored according to the second smallest eigenvalue of the Jacobian matrix (λ_2). **(c)** The space of intrinsic growth rates ($\mathbf{r}$) for the same system shown in (a) and (b) colored according to the distance to closest border ($\min\{d_b\}$) of the feasibility domain, which are indicated as black curves. Note that $\mathbf{r}$-vectors on the feasibility domain are normalized to unit norm (i.e., $||\mathbf{r}|| = 1$). **(d)** The same space of intrinsic growth rates, but colored according to the distance to closest vertex ($\min\{d_v\}$) of the feasibility domain.

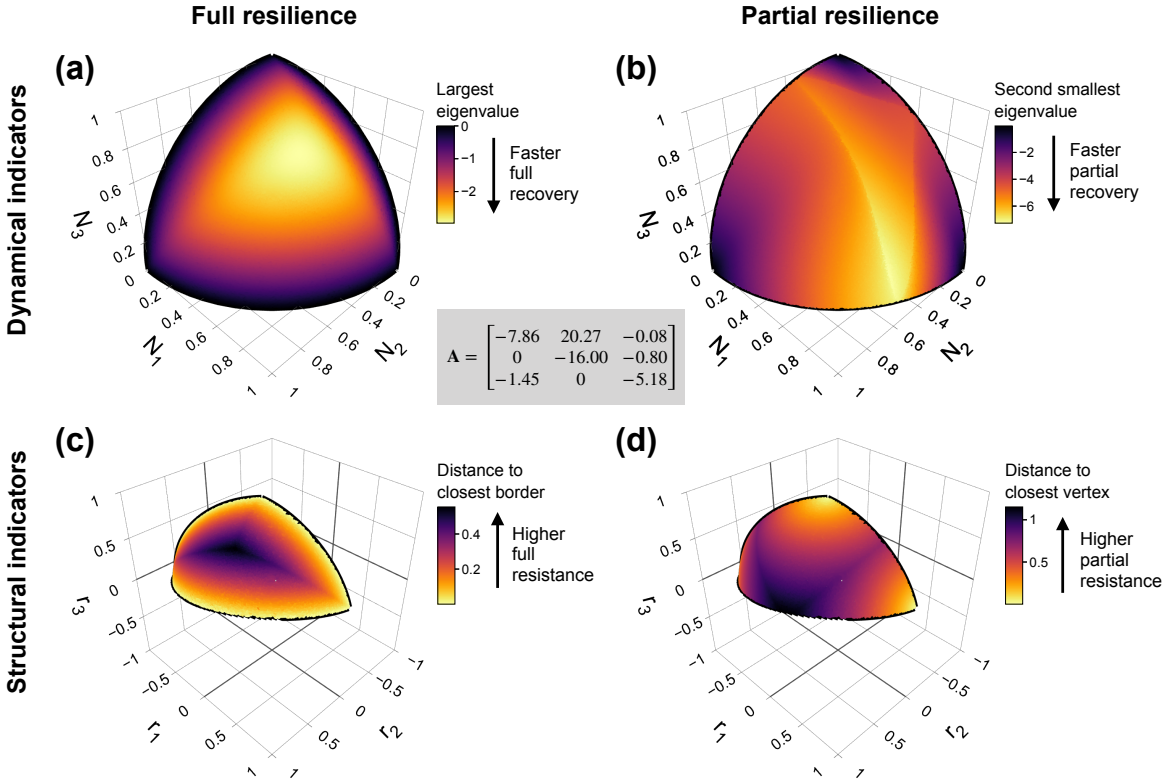

Figure S10: Dynamical and structural indicators of full and partial resilience in a competition/antagonistic microbial system (system 9: Pa-Pci-Pv; Tables S1 and S3). **(a)** The 3-dimensional space of species abundances at equilibrium ($\mathbf{N}^*$) colored according to the largest eigenvalue of the Jacobian matrix (λ_1). The interaction matrix $\mathbf{A}$ of this 3-species system is shown in the center of the figure. Note that this space corresponds to the positive orthant of the unit sphere (i.e., $||\mathbf{N}^*|| = 1$, $N_i^* > 0 \; \forall \; i$). **(b)** The same space of species abundances, but colored according to the second smallest eigenvalue of the Jacobian matrix (λ_2). **(c)** The space of intrinsic growth rates ($\mathbf{r}$) for the same system shown in (a) and (b) colored according to the distance to closest border ($\min\{d_b\}$) of the feasibility domain, which are indicated as black curves. Note that $\mathbf{r}$-vectors on the feasibility domain are normalized to unit norm (i.e., $||\mathbf{r}|| = 1$). **(d)** The same space of intrinsic growth rates, but colored according to the distance to closest vertex ($\min\{d_v\}$) of the feasibility domain.

References

Friedman, J., Higgins, L.M. & Gore, J. (2017) Community structure follows simple assembly rules in microbial microcosms. *Nature Ecology and Evolution* **1**, 0109.